


RESEARCH

Open Access



Phosphorylation sites of microtubule-associated protein 1B (MAP 1B) are involved in axon growth and regeneration

Yuya Ishikawa^{1,2}, Masayasu Okada^{2,3,4}, Atsuko Honda², Yasuyuki Ito², Atsushi Tamada^{2,3,5}, Naoto Endo¹ and Michihiro Igarashi^{2,3*} 

Abstract

The growth cone is a specialized structure that forms at the tip of extending axons in developing and regenerating neurons. This structure is essential for accurate synaptogenesis at developmental stages, and is also involved in plasticity-dependent synaptogenesis and axon regeneration in the mature brain. Thus, understanding the molecular mechanisms utilized by growth cones is indispensable to understanding neuronal network formation and rearrangement. Phosphorylation is the most important and commonly utilized protein modification in signal transduction. We previously identified microtubule-associated protein 1B (MAP 1B) as the most frequently phosphorylated protein among ~ 1200 phosphorylated proteins. MAP 1B has more than 10 phosphorylation sites that were present more than 50 times among these 1200 proteins. Here, we produced phospho-specific antibodies against phosphorylated serines at positions 25 and 1201 of MAP 1B that specifically recognize growing axons both in cultured neurons and in vivo in various regions of the embryonic brain. Following sciatic nerve injury, immunoreactivity with each antibody increased compared to the sham operated group. Experiments with transected and sutured nerves revealed that regenerating axons were specifically recognized by these antibodies. These results suggest that these MAP 1B phosphorylation sites are specifically involved in axon growth and that phospho-specific antibodies against MAP 1B are useful markers of growing/regenerating axons.

Keywords: Phosphorylation, MAP 1B, Development, Growth cone, Axon regeneration

Introduction

The growth cone is a specialized motile structure that forms at the tip of growing axons of developing neurons and plays a role in accurate synaptogenesis for neuronal network construction [1]. The molecular basis of the mammalian growth cone is poorly understood due to its high complexity. However, recent approaches using proteomics, which quantitatively identifies proteins [2, 3], have gradually contributed to new views of axon growth (for example, [4–6]).

Microtubule-associated protein 1B (MAP 1B) [7–9] functions as a microtubule (MT)-stabilizing protein in

developing neurons [10–12] and is highly expressed at various stages of axogenesis [13, 14]. MAP 1B interacts with actin and other regulators of MTs [15–17]. Among microtubule-associated proteins, MAP 1B is the most abundant cytoskeletal protein in the growth cone, as identified by proteomics, except for tubulin and actin [1–3]. In addition, phosphorylation of MAP 1B is involved in axon growth/regeneration and plasticity [18, 19]. Thus, identification of MAP 1B phosphorylation sites and investigation of their roles in axon formation should contribute to the understanding of nerve growth/regeneration mechanisms.

Phosphoproteomics is a new method for comprehensive identification of the phosphorylation sites of proteins [20]. We recently reported results of a phosphoproteomics study of the growth cone membrane (GCM) and revealed that the most frequent phosphorylation sites in GCM are in MAP 1B [21]. Two proline-directed sites for phosphorylation,

* Correspondence: tarokaja@med.niigata-u.ac.jp

²Department of Neurochemistry and Molecular Cell Biology, Graduate School of Medical and Dental Sciences, Niigata University, 1-757 Asahimachi, Chuo-ku, Niigata 951-8510, Japan

³Trans-disciplinary Research Programs, Brain Research Institute, Niigata University, Niigata, Japan

Full list of author information is available at the end of the article



S25 and S1201, in MAP 1B are the most abundant in MAP 1B, and are also highly frequent among the total phosphorylated sites of ~ 1200 proteins.

Here, we focused on these two sites and produced phospho-specific antibodies (Abs) against them. Both sites were regulated during development, and the Abs recognized growing axons *in vivo* in various regions of the developing mouse brain. In addition, immunoreactivity for S25 and S1201 also emerged as early as 6 h after sciatic nerve injury and in distally regenerating axons that have extended past the injury point.

Taken together, we conclude that these sites are closely related to axon growth and regeneration, and that the Abs are potential molecular markers of growing/regenerating axons.

Results

Both pS25 and pS1201 abs recognized growing axons in the developing brain

We produced phospho-specific Abs against MAP 1B phospho-peptides (Additional file 1: Figure S1A). Mutated peptides including S25A or S1201A were not recognized by the phospho-S25 (pS25) or the phospho-S1201 (pS1201) Abs, respectively (Additional file 1: Figure S1B), indicating that these Abs specifically reacted with phosphorylated S25 and S1201, respectively.

pS25 (Fig. 1a) and pS1201 (Fig. 1b) Abs preferentially labeled the axons of cultured neurons, and each Ab showed stronger immunoreactivity to the axon than the MAP 1B Ab (Fig. 1c). We measured the intensity of the distal portion of the axon after linearizing the axon (Fig. 1d), and the ratios to MAP 1B itself were calculated. The intensities of pS25 and pS1201 immunoreactivity distally along the axon were similar to each other (Fig. 1e). pS25 or pS1201 immunoreactivity was colocalized with MTs, rather than F-actin, and these Abs recognized the distal axon of the growing neurons (Fig. 1f-g).

Immunoreactivity for both pS25 and pS1201 was distributed similarly to tubulin (Fig. 2a-h), and was quantitatively enriched in the MT area, but not the F-actin area (Fig. 2i). A biochemical co-sedimentation assay for MT binding affinity using an extract of E15 mouse brain showed that immunoreactivity for both Abs was collected in the MT fraction (Fig. 2j), suggesting that these phosphorylation sites are related to the interaction between MAP 1B and MTs. SMI-31 immunoreactivity, which mainly recognizes the phosphorylated neurofilament protein-H and partially recognizes phospho-MAP 1B [22], was similar but not identical to that of pS25 and pS1201, suggesting that SMI-31 has a different specificity from pS25 or pS1201 (Additional file 1: Figure S2).

Using specific inhibitors for c-Jun *N*-terminal kinase (JNK) and glycogen synthase kinase 3 β (GSK3 β), we determined the responsible protein kinase and found that

pS25 was specifically inhibited by JNK inhibitors but not GSK3 β inhibitors. In contrast, pS1201 was inhibited by both types of inhibitors (Additional file 1: Fig. S3).

These Abs also preferentially recognized bundles of axons with *in vivo* immunohistochemistry of sagittal sections of E15 mouse brain (Fig. 3a). Compared to the L1 Ab and DAPI reactivity, pS25 and pS1201 Abs labeled developing axons (Fig. 3b-d). Immunoreactivity of each Ab against pS25 and pS1201 was mainly and highly expressed at developmental stages and rapidly decreased in the mature brain (Fig. 3e-f).

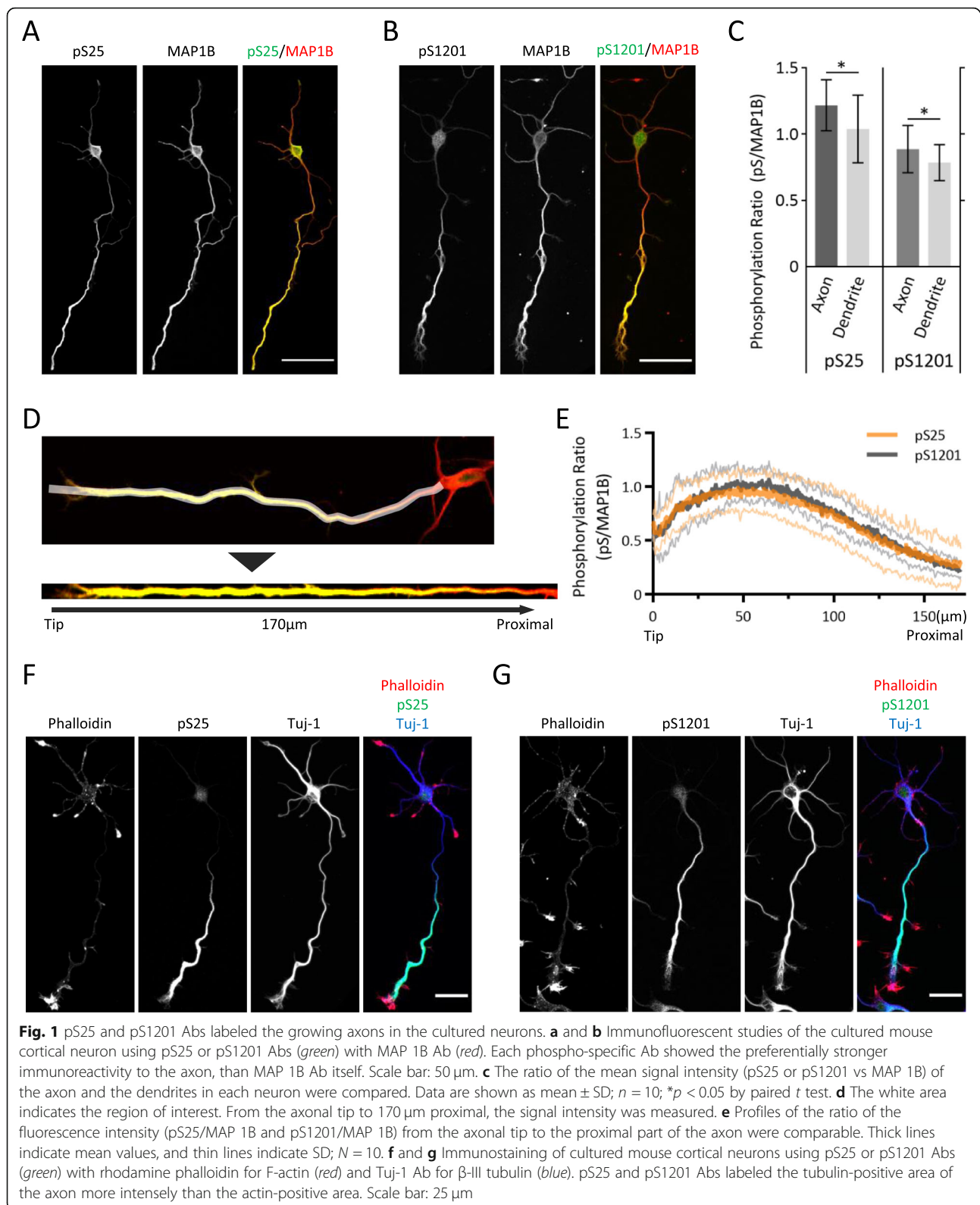
In various regions of the embryonic mouse brain, these Abs also labeled growing axon bundles *in vivo* (Fig. 4). Taken together, these MAP 1B phospho-specific Abs specifically label growing axons at various stages of development.

pS25 and pS1201 are maintained in regenerating axons after sciatic nerve injury

Next, we examined whether these phosphorylation sites serve as molecular markers of regenerating axons as well as GAP-43 pS96 [21]. We chose the crushed sciatic nerve injury as a model of axon regeneration [21]. As a positive control, we used immunoreactivity for SCG10, a protein that inhibits tubulin polymerization in developing neurons. Six hours after the crush injury, both phosphorylated S25 and S1201 were upregulated in the injury site and were co-expressed with SCG10 (Fig. 5a-c). Two days after injury, both areas of phosphorylation had extended to the distal side past the injury point, similar to SCG10 Ab immunoreactivity (Fig. 5a-c). Quantitative analysis revealed that the area recognized by each phospho-specific Ab was increased by more than 10-fold (Fig. 5d). Although expression of MAP 1B itself was upregulated in the crushed nerves, the variance of the signal intensity was not sufficient for calculating the regeneration index (Additional file 1: Figure S4).

We analyzed the distribution patterns of these phosphorylated sites using a different method of injury, namely, transection of the sciatic nerve (Fig. 6).

On day 1 after injury, the proximal segments of the transected nerves showed high immunoreactivity with pS25 and pS1201 Abs compared to the distal segments and the intact nerves (Fig. 6a-b). On day 3, high immunoreactivity for pS25 and pS1201 was maintained in the proximal segments (Fig. 6a-b), but not in the distal ones (Fig. 6a-b). In contrast to pS25 and pS1201, immunoreactivity with a pan-MAP 1B Ab showed only a slight change after nerve transection (Fig. 6c). Increased expression of SCG10 was detected in the proximal segment of the transected nerve on day 1 and was maintained on day 3 (Fig. 6d). Similarly, pS25 and pS1201 immunoreactivity, as well as MAP 1B itself, was maintained (Fig. 6a-c and Fig. 6g), suggesting that the phosphorylation sites at S25



and S1201 in the proximal segment are involved in axon regeneration events. Quantitative analysis confirmed this hypothesis (Fig. 6e, f, and h).

Finally, we examined the effects of sciatic nerve injury caused by suturing (Fig. 7). The sutured nerves showed stronger immunoreactivity with pS25 and pS1201 Abs

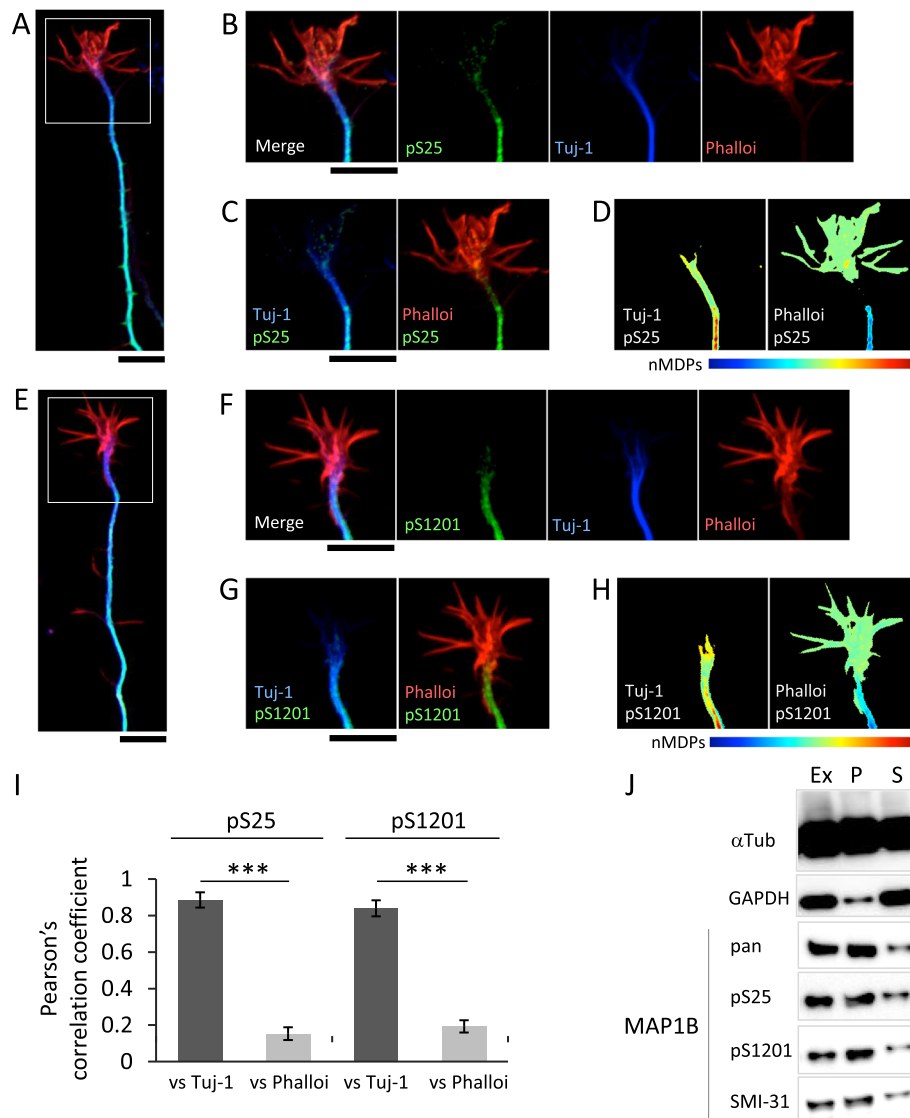


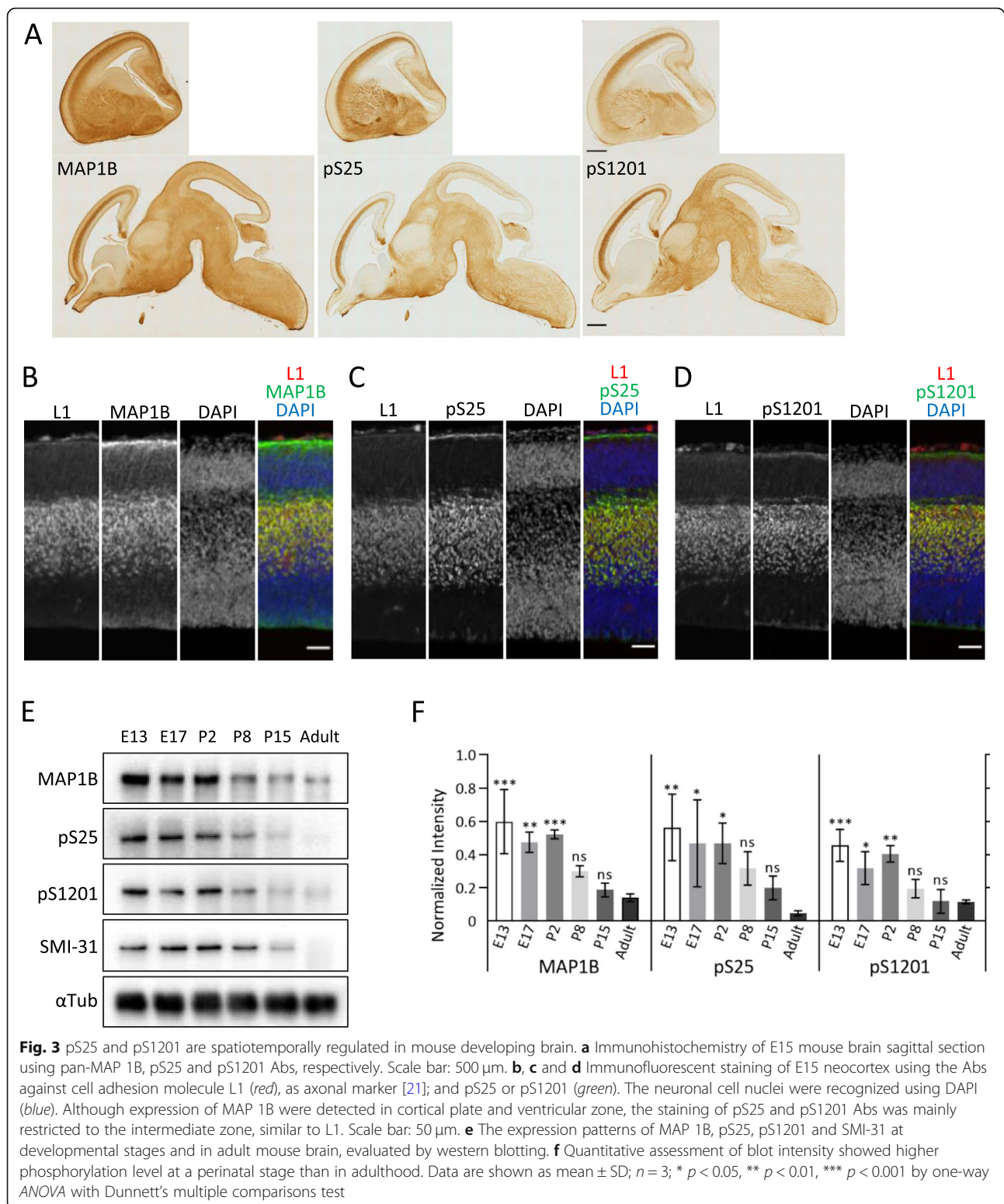
Fig. 2 pS25- and pS1201 MAP 1B bind to axonal MTs. **a-h** Immunostaining images of Tuj1 (blue) /phalloidin (red) /pS25 (green: **b-d**), or pS1201 (green: **f-h**) in the axonal growth cone of 3DIV mouse cortical neurons. High magnificant images in ROI (**a** or **e**) are shown (**b-d**) or (**f-h**), respectively. Images of normalized mean deviation product (nMDP) (**d**, **h**; see *Materials and Methods*) from the double staining, Phalloidin/pS25 (**c**) and Tuj1/pS25 (**d**); phalloidin/pS1201 (**g**) and Tuj1/pS1201 (**h**). Tuj1/pS25 and Tuj1/pS1201 show strong co-localization in axons (cyan in the merged images and hot colors in the nMDP images), although both phalloidin/pS25 and phalloidin/pS1201 show weak or no colocalization (cold colors in the nMDP images). Scale bars, 3 μ m. **i** Quantification of colocalization between the phosphorylated MAP 1B (pS25 or pS1201) and cytoskeletons (tubulin and F-actin) in the axonal growth cone ($n = 10$ for each; $***p < 0.001$). Data are presented as mean \pm SD. Student's *t*-test. **j** Determination of MT binding affinities by the co-sedimentation assay, using an extract of E15 mouse brains. Ex: extract; P: pellets; and S: supernatant

than the non-sutured distal segment (Fig. 7a-b), similar to the SCG10 Ab (Fig. 7c). Namely, in the distal segments of the ligated nerves, the regenerating axons that had penetrated through the repair site were labeled with pS25 and pS1201 Abs (Fig 7a-b). The immunoreactivity with each phospho-specific Ab was significantly more concentrated in the sutured distal segment than in the non-sutured segment (Fig. 7d).

These results suggest that the phospho-specific Abs against pS25 and pS1201 of MAP 1B specifically label regenerating axons.

Discussion

The MAP 1B phosphorylation sites S25 and S1201 are newly characterized in this paper. These two sites were identified by our phosphoproteomics analysis as



highly frequent sites among ~ 5000 identified ones [21]. However, the significance of phosphorylation at these sites had not been examined well. Developmentally, such

mitogen-activated protein kinase signaling pathways are involved in axon formation via MAP 1B phosphorylation [24–26], suggesting that these new

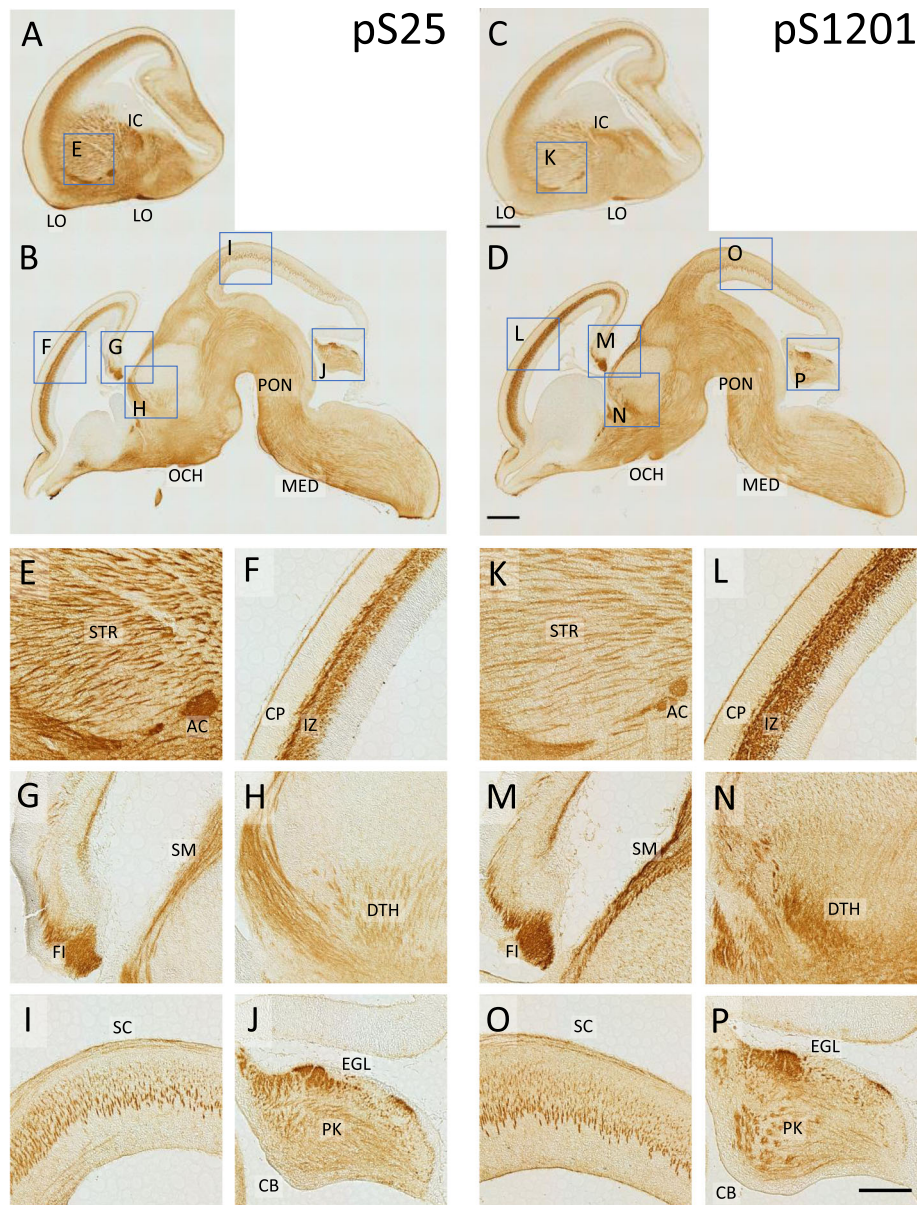


Fig. 4 Immunohistochemistry of various brain regions in E15 mouse, using pS25 and pS1201 Abs. Microscopic images of sagittal sections derived from various regions were DAB-stained using pS25 (**a, b, e-j**) or pS1201 Abs (**c, d, k-p**). Boxes in (**a-d**) represent the regions enlarged in (**e-p**), respectively. Both pS25 and pS1201 Abs succeeded in labelling the bundles of nerve fibers, such as internal capsule, lateral olfactory tract (**a, c**), optic chiasm (**b, d**), anterior commissure (**e, k**), fimbria of hippocampus, and stria medullaris (**g, m**). In the neocortex, the intermediate zone, where the developing axons are enriched, was specifically labelled (**F, L**). Fibers in striatum (**e, k**), dorsal thalamus (**h, n**), superior colliculus (**i, o**), and cerebellum (**j, p**) were also labelled. The scale bar: 500 μ m (**c, d**; in **a-d**), 200 μ m (**p**; in **e-p**), respectively. *Abbreviations*: AC, anterior commissure; CB, cerebellum; CP, cortical plate; DTH, dorsal thalamus; EGL, external granular layer; FI, fimbria of hippocampus; IC, internal capsule; IZ, intermediate zone; LO, lateral olfactory tract; MED, medulla; OCH, optic chiasm; PK, Purkinje cell layer; PON, pons; SC, superior colliculus; SM, stria medullaris; STR, striatum

phosphorylated sites were worth examining for a relationship to axon development. In addition, because of our GAP-43 S96 studies [21], we suspected that these sites are likely to be involved in axon regeneration in the adult.

pS25 and pS1201 of MAP 1B during development

Compared with MAP 1B itself, these phosphorylation sites were enriched in distal axons and growth cones (Fig. 1a-b), suggesting that S25 and S1201 phosphorylation sites are involved in the localization of MAP 1B at

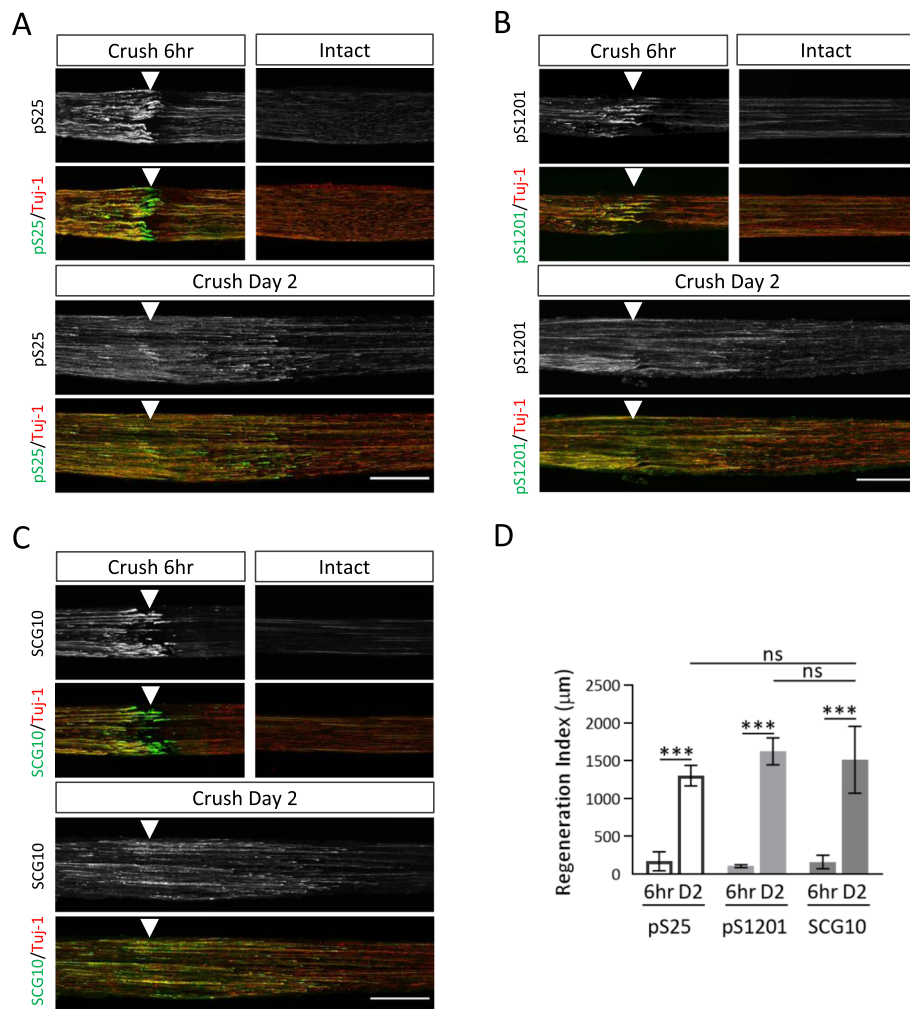


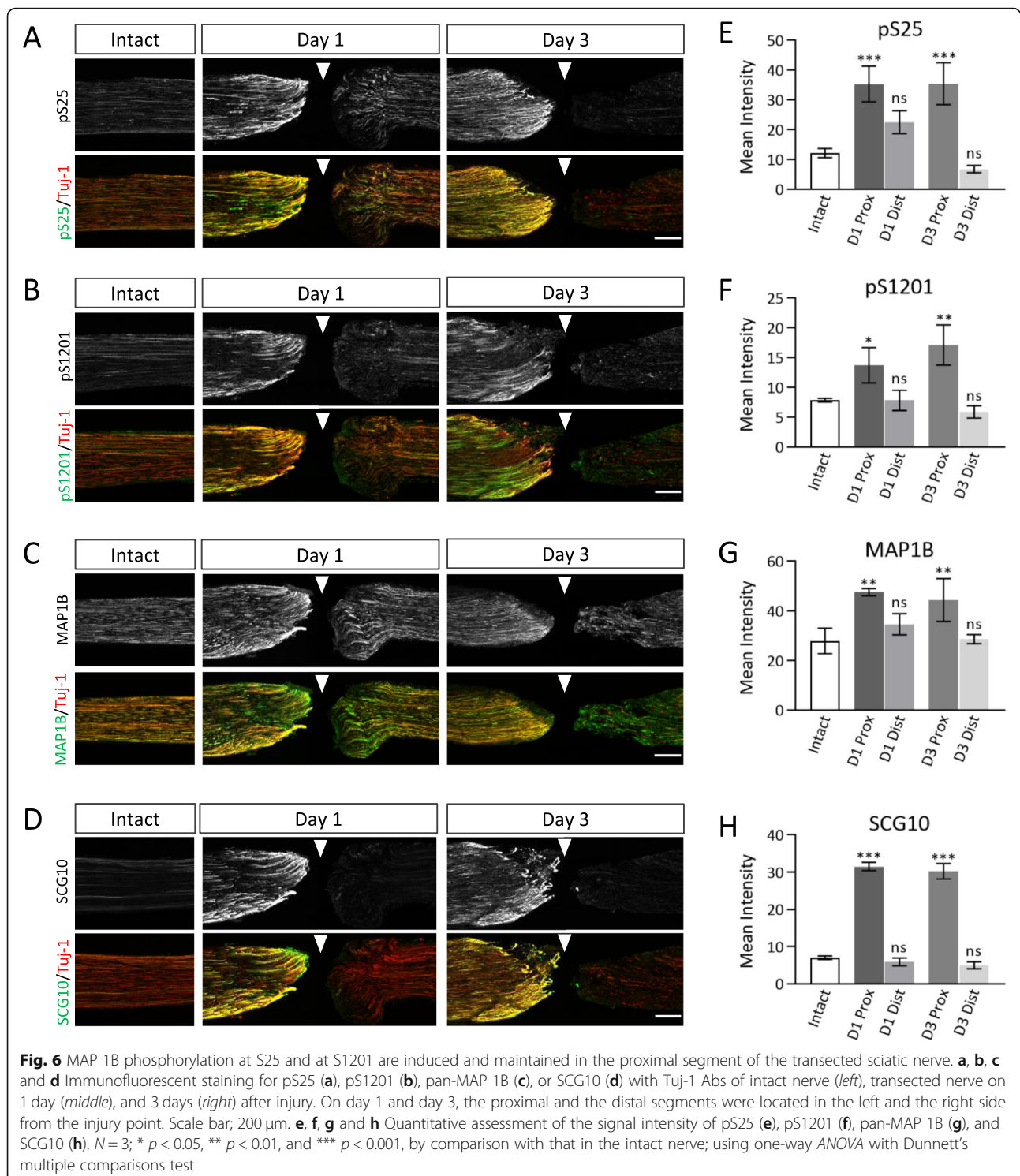
Fig. 5 Phosphorylation of S25 and S1201 are involved in the peripheral nerve injury in adult mouse. **a, b and c** Immunofluorescence of mouse longitudinal sciatic nerve sections, using pS25 (**a**), pS1201 (**b**), or SCG10 (**c**) Abs (each green) and Tuj-1 (red) Ab, at 6 h or in 2 days after injury. The proximal side (left) and the injured point (arrowhead) are shown. Intact: sham operation in the other side of the injured nerve. Scale bar: 500 µm. **d** Regeneration index [23], which is the distance from crush site to the location that the signal level of target object decreases to the half of the crush site, of pS25 and pS1201 was higher on 2 days after crush than on 6 h after crush. The index of pS25 and pS1201 was similar to the index of SCG10. $N = 3$ (6 h) and $n = 3$ (2 d); *** $p < 0.001$ by one-way ANOVA with Sidak's multiple comparisons test

the distal portions of the axon in developing neurons. These two sites were distributed similarly to each other according to quantitative analysis (Fig. 1d-g).

The phosphorylation sites, S25 and S1201, are located within the actin-binding domain and the MT-assembly helping domain, respectively [12]. The former domain is thought to be related to the association between MTs and F-actin, and the latter is closely involved in stabilization of MTs [12]. Thus, we examined whether these sites are related to MTs or F-actin bundles. Quantitative analysis revealed that these phosphorylation sites were colocalized with MTs (Fig. 2c and g), rather than F-actin (Fig. 2d and h; also see Fig. 2i), and they co-sedimented with MTs (Fig. 2j), indicating that pS25 and

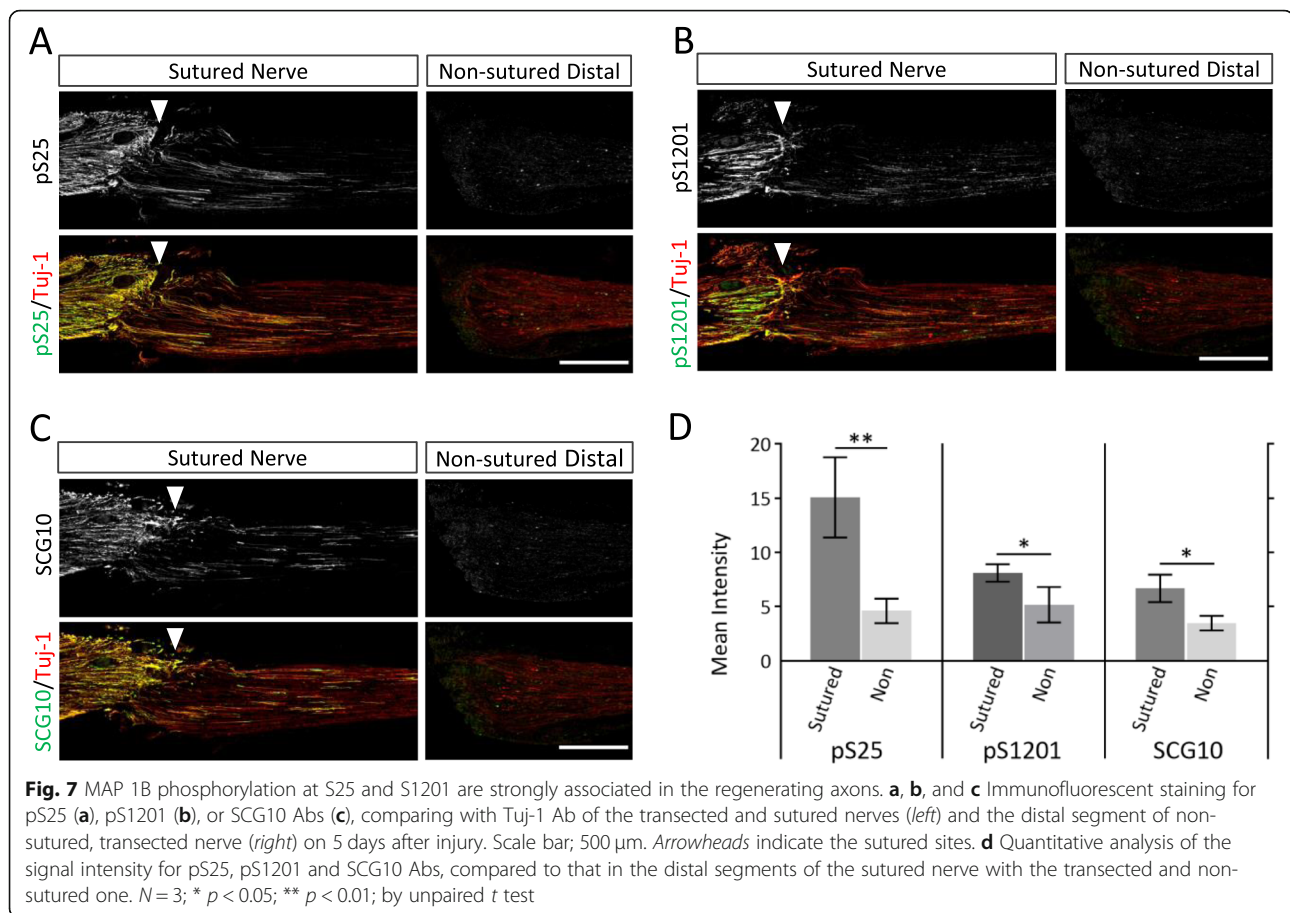
pS1201 are involved in MT binding, but not interactions with F-actin.

Phosphorylation of S25 and S1201 were developmentally regulated and mainly expressed at embryonic stages (Fig. 3e-f), although MAP 1B itself is also expressed during these stages. When considering the distribution and developmental expression patterns, S25 and S1201 phosphorylation seems consistent with the previously described "Mode I", which was reported to be reduced during development more than two decades ago [18, 27, 28]. "Mode I" phosphoproteins are also localized in the distal portion of axons and growth cones, features that are totally consistent with S25 and S1201 (Fig. 3a-b). SMI-31, which previously was used to characterize "Mode I" phosphorylation, is a



monoclonal Ab that mainly recognizes phosphorylation of the high-molecular-weight subunit of neurofilament protein in the adult [22, 29], but also recognizes phosphorylated MAP 1B [30, 31]. The distribution of SMI-31 immunoreactivity was similar but not identical to that with pS25/pS1201 Abs (Additional file 1: Figure S2C-D), and

the developmental patterns of SMI-31 were not equal to those of pS25/pS1201 Abs (Fig. 2e), suggesting that SMI-31 recognizes a different epitope than these phosphorylated MAP 1B Abs. Since the previous studies using SMI-31 for Mode-I phosphorylation mainly used the rat brain [27, 28] and ours uses the



mouse, there seem the spatial and temporal discrepancies between them due to the species difference. In addition, further investigations will be needed to examine whether SMI-31 also recognize these phosphorylation sites.

We previously demonstrated that JNK is responsible for phosphorylation of P-directed substrates in growth cones, which occupy a large proportion of phosphorylation sites in growth cones as revealed by phosphoproteomics [21]. Here, we used several inhibitors of both JNK and GSK3 β . As a result, phosphorylation of S25 was specifically inhibited by JNK inhibitors but not GSK3 β inhibitors. However, phosphorylation of S1201 was inhibited by both types of inhibitors (Additional file 1: Figure S3), suggesting that JNK phosphorylates both phospho-sites but GSK3 β is involved in only S1201 phosphorylation at developmental stages. This is consistent with previous reports on growing/regenerating axons [32, 33].

Growing axons were specifically labeled by pS25 and pS1201 Abs with in vivo immunohistochemistry in various regions of the developing brain (Fig. 3a-d and Fig. 4). Judging from the phosphoproteomics data of GCM showing that S25 and S1201 are highly frequent sites of MAP 1B phosphorylation [21], these results indicate that S25 and S1201 are the major sites of “Mode I”

phosphorylation in vivo, and that as for the phospho-specific Abs, which recognize the specific phosphorylation sites as their specified epitopes (Additional file 1: Figure S1B), pS25/pS1201 Abs are much better markers for “Mode I” than SMI-31.

pS25 and pS1201 of MAP 1B during axon regeneration

Axon regeneration is an important event during repair after injury, and whether mammalian axons can be successfully regenerated or not is an important medical problem [34]. We have postulated that GAP-43 pS96 Ab is a molecular marker of both growing and regenerating axons [21, 35] using the sciatic nerve injury model. Including our previous results that these phosphorylation sites were enriched in GCM, because MAP 1B phosphorylation is related to axon regeneration [36, 37], we suspected that pS25/pS1201 Abs would be potential markers of regenerating axons.

Crushed axons in the sciatic nerve were labeled by these two phospho-specific MAP 1B Abs past the injury point (Fig. 5), as well as by the SCG10 Ab, suggesting that these phosphorylation sites are in part related to axon regeneration. In addition, phosphorylated forms of these sites were concentrated in the proximal end of the

transected sciatic nerve (Fig. 6a-b, e-f), as was SCG10 (Fig. 6d and h), implying that the injury response may be transferred to the cell body and that phosphorylated MAP 1B may undergo anterograde axonal transport toward the injury site (Fig. 6a-b).

The sutured nerve experiments revealed that these phosphorylated forms of MAP 1B moved distally past the injury point (Fig. 7a-b, d). These forms may be transported anterogradely and be closely involved in axon regeneration, as is SCG10, a molecular marker of this event (Fig. 7c-d). These phosphorylated forms in the injury experiments may selectively undergo anterograde axonal transport to stimulate MT synthesis and stabilization in regenerating axons [38].

SCG10, a member of stathmin family, forms T₂S (tubulin dimer-stathmin) complexes and sequesters tubulin, and subsequently, SCG10 inhibits MT formation [39, 40]. SCG10 is related to axon growth via its ability to destabilize MTs [41–43] and is enriched in growth cones, as shown using proteomics [1–3]. Both SCG10 and pS25/pS1201 of MAP 1B were involved in axon regeneration (Figs. 5–7), suggesting that MT remodeling by these proteins in both directions may facilitate this event.

A regeneration index was measured based on SCG10 immunoreactivity to evaluate axon regeneration [23]. The regeneration indices of pS25 and pS1201 were similar to that of SCG10 (Fig. 5). Thus, these two phospho-specific Abs against MAP 1B may be useful for measuring the “regeneration index” [23]. SCG10 is expressed and highly phosphorylated mainly in developmental stages [21, 44], depolymerizes MTs, and regulates them in an opposite manner than MAP 1B. However, both are necessary for axon development and probably regeneration. Dynamic MTs are thought to be essential to growing/regenerating axons, and these two proteins are needed for dynamic regulation of MTs in both directions [45, 46]. Judging from our results, pS25 and pS1201 are likely to be involved in MT dynamics, and in the next step, how these two phosphoproteins, MAP 1B and SCG10 dynamically regulate MT organization in the growing axon, should be directly elucidated.

Finally, the functional understanding of these phosphorylation sites still remained to be elucidated. We showed here that phosphorylated forms at S25 and S1201 of MAP 1B are enriched in the growth cone and the distal axons (Figs. 1–3), and regulated during development (Fig. 4), suggesting that phosphorylation at these sites will greatly contribute to rapid axon formation, including after injury when axon regeneration is required.

As a next step, the molecular interactions that occur via these sites and colocalization of these molecules with phospho-MAP 1B should be clarified to increase our understanding of the regulatory mechanisms of axonal MT dynamics in these events. Superresolution microscopic

techniques and the use of our Abs will increase our understanding of how MTs (and F-actin) are regulated in growth cones when axons grow due to phosphorylation at these sites of MAP 1B [1, 4, 47, 48]. In addition, evolutionary analysis of the phosphorylation sites should elucidate important aspects of each phosphoprotein and phosphorylation site and will be helpful for further functional analysis of them [49, 50].

Materials and methods

Animals

All of the animal experiments were performed following approval from the Animal Resource Center of Niigata University. Pregnant ICR mice were purchased from Japan-SLC, Inc. (Shizuoka, Japan) and used for neuronal cell culture, immunostaining of embryonic mouse brain, and analysis of protein expression and phosphorylation levels in developing brain. Adult C57BL/6N mice were used for the experiments with sciatic nerve injury.

Abs

The Abs used in this paper and their dilutions are listed in Additional file 2: Table S1. The pS25 and pS1201 Abs were produced as previously described [21].

Plasmid construction

Inverse PCR-based mutagenesis techniques for the addition of a 2 × FLAG (DYKDDDDK) tag to the N-terminus of the rat *MAP 1B* sequence in the pMT5CMV vector [51, 52], a gift from Dr. F. Propst (Department of Biochemistry and Cell Biology, Max F. Perutz Laboratories, University of Vienna, Vienna, Austria), were performed using the KOD-Plus-Mutagenesis Kit (Toyobo Co., Ltd., Osaka, Japan) and the following primers: 2xFlag-pMT5-F (5'-ATGATGGATTACAAGGATGACGACGATAAGGATTACAAGGACGACGACGACAAGGGACTAGTCGCCACC-3') and 2xFlag-pMT5-R (5'-AGTCAATTGTGCGACGCGGCCGC-3'). To generate phosphorylation site mutations of *MAP 1B* (S25A, S1201A), inverse PCR-based mutagenesis techniques were also performed using the following primers: S25A sense (5'-ACCGCACCCAGCCTGTGCAC-3'); S25A antisense (5'-GGTCGCCGCCGGGTTGC-3'); S1201A sense (5'-ATAGCACCCACTTCGTCCATGGAAGAAGAC-3'); and S1201A antisense (5'-GGTGGAGGCGGAAGCGTTGTAATC-3').

Transfection of COS-7 cells and immunoprecipitation assay

Transfection experiments using COS-7 cells were performed as described previously [5]. Each plasmid expressing 2 × FLAG-tagged wild type, S25A, or S1201A full-length *MAP 1B* were transfected using PEI 'MAX' (Polysciences, Inc., Warrington, PA, USA). After 48 h, the

transfected cells were lysed with lysis buffer (1% NP-40, 50 mM Tris-HCl [pH 7.5], 150 mM NaCl) containing protease inhibitors (10 µg/ml leupepsin, 10 µg/ml pepstatin A, and 0.1 mM p-APMSF) and phosphatase inhibitors (20 mM NaF and 1 mM Na₃VO₄), sonicated, and centrifuged at 12,000×g at 4 °C. To each supernatant, 2 µg anti-DDDDK-tag mAb (clone FLA-1, Medical & Biological Laboratories Co., Ltd., Aichi, Japan) was added, and the mixture was incubated at 4 °C for 3 h. In addition, 25 µl Protein G Mag Sepharose slurry (GE Healthcare UK, Ltd., Buckinghamshire, UK) was mixed and incubated at 4 °C for 1 h and eluted with 1 × sample buffer for SDS-PAGE.

Western blotting and analysis of the MAP 1B phosphorylation levels

Protein samples were separated by SDS-PAGE in 6% gel or 4–20% polyacrylamide gradient gel, soaked in transfer buffer and electroblotted onto PVDF membrane overnight. The membrane was incubated with primary Abs for 90 min and with HRP conjugated secondary Abs for 30 min at room temperature. Protein bands were visualized with an ECL Prime kit (GE Healthcare UK, Ltd.). For developmental analysis of MAP 1B, the whole brains of E13, E17, postnatal day (P) 2, P8, P15 and adult mice were homogenized in lysis buffer with protease inhibitors and phosphatase inhibitors and centrifuged at 12,000×g at 4 °C. Half volume of 3 × sample buffer for SDS-PAGE was added to each supernatant. To analyze the expression or the phosphorylation level of MAP 1B, ImageJ software Fiji (<http://rsb.info.nih.gov/ij>) was used to measure the areas under the curve of the immunoblotted bands. In the developmental analysis, the values were normalized to α-tubulin Ab and compared to that of adult brain, which was defined as 1.0.

Neuronal cell culture

The cerebral cortex neurons of E15 mice were cultured, as described previously [4, 6, 21]. For the inhibition assay of MAP 1B phosphorylation, 4 days in vitro (DIV) cortical neurons were treated for 24 h with culture medium containing DMSO as a control, one of three JNK1 inhibitors [SP600125, JNK Inhibitor V, and JNK Inhibitor XVI (Cayman Chemical, USA)], or one of three GSK3β inhibitors [IM-12, TDZD-8 (Cayman Chemical, USA), and LiCl (99.5% purity, Wako, Osaka, Japan)]. Cells exposed to each inhibitor were lysed in 1 × SDS-PAGE sample buffer and processed for western blotting analysis.

Immunofluorescent staining and image analysis

The 3–4 DIV cortical neurons were fixed for 15 min with 4% paraformaldehyde (PFA) in PBS, permeabilized using 0.1% TritonX-100 in PBS and incubated in 3% BSA/PBS for blocking. The cells were incubated with primary Abs diluted in 1% BSA/PBS overnight at 4 °C, and

then incubated with secondary Abs (Jackson ImmunoResearch Inc., West Grove, PA, USA; 1/1000 dilution), for 30 min at room temperature, and mounted in Fluorescence Mounting Medium (Agilent Technologies, Inc., Santa Clara, CA, USA). Samples were observed using a confocal microscope (FV1200; Olympus, Tokyo, Japan). For the line plot analysis of axons, the longest neurite defined as an axon, and the second longest neurite, defined as dendrite were outlined with the ROI tool of ImageJ. The mean intensities of the fluorescence in each ROI were measured. The immunopositive ratios of pS25 or pS1205 Abs to pan-MAP 1B Ab in an axon and a dendrite were calculated, and the ratios of axon was compared to that of dendrite, which was defined as 1.0. For the colocalization assay, values of either the normalized mean deviation product or Pearson's correlation coefficient (R value) were calculated with the plug-ins of ImageJ/Fiji software, Colocalization Colormap [53] or coloc2, respectively.

MT co-sedimentation assay

The MT co-sedimentation assay was performed according to the method described in [54] with modifications. E15.5 mouse brains were homogenized in assembly buffer (100 mM MES, 0.5 mM MgCl₂, 1 mM EGTA, pH 6.8) containing 1 mM DTT, 1 mM APMSF, 1 µg/ml pepstatin A, 1 µg/ml leupeptin, 1 mM Na₃VO₄, 1 mM NaF, 1 mM Na₂MoO₄, and 2 mM imidazole, with a glass-Teflon homogenizer. The homogenate was centrifuged at 30,000×g for 1 h at 4 °C, and crude extract was mixed with glycerol (1/3 volume of the total extract) and 1 mM GTP (final concentration). After incubation at 37 °C for 40 min, MTs and MT-associated proteins were collected by centrifugation at 100,000×g for 40 min at 37 °C. The pellets were then re-suspended in the assembly buffer with the same volume as the supernatant.

Immunohistochemistry of mouse embryonic brain

Immunohistochemistry with phospho-specific MAP 1B Abs on embryonic mouse brain was performed as described previously [21]. In brief, brains of E15 mice were fixed with 4% paraformaldehyde in 0.1 M phosphate buffer (pH 7.4) for 1 d at 4 °C and cryoprotected with 30% sucrose in 0.1 M phosphate buffer. Specimens were immersed in a solution consisting of OCT compound (Sakura Finetechnical Co., Ltd., Tokyo, Japan) and 30% sucrose/0.1 M phosphate buffer and embedded by freezing in ethanol cooled with dry ice. Sagittal sections were sliced at a thickness of 20 µm using a sliding cryotome (CM1850; Leica Biosystems, Wetzlar, Germany) and thaw-mounted on MAS-coated slide glass (Matsunami Glass Inc., Ltd., Osaka, Japan).

For diaminobenzidine staining, slides were incubated with methanol containing 0.3% H₂O₂ for 30 min, washed with 0.2% Triton X-100 in PBS (PBST), and then

incubated overnight with primary Abs diluted in 1% BSA/PBST. On the next day, the slides were reacted with *N*-Histofine Simple Stain Mouse MAX PO (R) (Nichirei Biosciences Inc., Tokyo, Japan), and brown color was developed using a diaminobenzidine substrate kit (Nichirei Biosciences Inc.). Images were acquired with an upright microscope (BX63; Olympus) equipped with differential interference contrast optics.

For multiple fluorescent staining, slides were incubated overnight with primary Abs diluted in 1% BSA/PBST, and then incubated with Alexa Fluor 488 Goat Anti-Rabbit IgG (H + L) Ab (1/500), Goat anti-Rat IgG (H + L) Cross-Adsorbed Secondary Ab, Alexa Fluor 594 (Life Technologies; 1/500), and 4', 6-diamidino-2-phenylindole, dihydrochloride (DAPI; Life Technologies; 1/5000). Fluorescent images were acquired with an upright microscope (BX63; Olympus).

Sciatic nerve injury

Female C57BL/6 N mice (3–5 months old) were anesthetized by intraperitoneal injection of a mixture of ketamine, xylazine, and pentobarbital, and the following three types of injury models were made: (Model 1) Using the protocol reported previously [23, 55], the right sciatic nerve was crushed with a fine forceps (Fontax, INOX #5) for 30 s, and the mice were sacrificed 6 h or 2 d after the operation. (Model 2) The right sciatic nerve was transected with surgical scissors, and the mice were sacrificed 1 or 3 d after the operation. (Model 3) The right sciatic nerve was transected and then repaired by end-to-end suturing using 10–0 nylon, and the mice were sacrificed after 5 d. In all three models, the left sciatic nerve underwent a sham operation. Three mice were used for each surgery.

For immunohistochemistry, the sciatic nerves were treated as described previously [21]. Alexa Fluor 488 Goat Anti-Rabbit IgG (H + L) Antibody (Jackson ImmunoResearch Inc.) and Streptavidin Alexa Fluor 594 conjugate (Life Technologies; 2 µg/mL) were used as the secondary Abs. To evaluate the regeneration index [21, 23], the intensity along the nerve was measured using a rectangular ROI with ImageJ. To measure the signal intensity, the nerve was outlined with the freehand ROI tool of ImageJ so that the area was 0.4 mm², and the mean intensity was measured. The regeneration index [23], which is the distance from the crush site to the location that the signal level of the target object decreases to half of that of the crush site, was calculated.

Statistics

All data are represented as mean values ± standard deviation (SD). Paired or unpaired Student's *t* tests or one-way analysis of variance (ANOVA) with Dunnett's or Sidak's post-hoc multiple comparison tests were performed using GraphPad Prism7 (GraphPad Software), and *p* < 0.05 was considered to be statistically significant.

Supplementary information

Supplementary information accompanies this paper at <https://doi.org/10.1186/s13041-019-0510-z>.

Additional file 1: Figure S1. The specificity of pS25 and pS1201 Abs. **Figure S2.** pS25 and pS1201 Abs labeled more specific parts of the axon than SMI-31 Ab. **Figure S3.** Inhibitor sensitivities of pS25 and pS1201. **Figure S4.** Fluorescent immunostaining of pan-MAP 1B in the sciatic nerve.

Additional file 2: Table S1. Abs used for immunodetection in this paper.

Abbreviations

Ab: Antibody; ANOVA: Analysis of variance; BSA: Bovine serum albumin; GCM: Growth cone membrane; GSK3β: Glycogen synthase kinase-3β; JNK: C-jun *N*-terminus kinase; MAP 1B: Microtubule-associated protein 1B; PBS: Phosphate-buffered saline; ROI: Region of interest; SD: Standard deviation

Acknowledgements

We thank Kei Watanabe, MD/PhD (Department of Orthopedic Surgery, Niigata University Medical and Dental Hospital), for his encouragement, discussion, and support; and Prof. Friedrich Probst for providing the MAP 1B expression vector.

Authors' contributions

Yshikawa, MO, AH, NE, and MI designed the experiments; Yshikawa and AH performed the experiments; Ylto and AT prepared the experimental materials and supported the experiments; MI and Yshikawa wrote the paper. All authors read and approved the final manuscript.

Funding

This work was supported in part by KAKENHI from JSPS and MEXT of Japan (#17023019, #22150003, #22240040, #24111515, #18H04670, and #18H04013 to M.I.; #17 K10926 to M.I. and Kei Watanabe; #17 K17739 to M.O.; #25870251 to A.K.; and #18 K06480 to A.H.), Takeda Science Foundation (to A.H. and to Y. Ito), Uehara Memorial Foundation for Life Sciences (to M.I. and Y. Ito), U-go grant from Niigata University (to A.H.), AMED-CREST (#19gm1210007s0101 to M.I.), and TERUMO Foundation for Life Sciences and Arts (#17-2b22 to A.H.).

Availability of data and materials

The phosphopeptides identified using phosphoproteomics for MAP 1B are shown in ref. [21] and its supplementary information files.

Ethics approval

All of the animal experiments were performed following approval from the Animal Resource Center of Niigata University.

Consent for publication

Not applicable.

Competing interests

The authors declare that they have no competing interests.

Author details

¹Division of Orthopedic Surgery, Department of Regenerative and Transplant Medicine, Graduate School of Medical and Dental Sciences, Niigata, Japan. ²Department of Neurochemistry and Molecular Cell Biology, Graduate School of Medical and Dental Sciences, Niigata University, 1-757 Asahimachi, Chuo-ku, Niigata 951-8510, Japan. ³Trans-disciplinary Research Programs, Brain Research Institute, Niigata University, Niigata, Japan. ⁴Department of Neurosurgery, Brain Research Institute, Niigata University, Niigata, Japan. ⁵Department of iPS Cell Applied Medicine, Kansai Medical University, Hirakata, Osaka 573-1010, Japan.

Received: 4 June 2019 Accepted: 10 October 2019

Published online: 11 November 2019

References

- Igarashi M. Molecular basis of the functions of the mammalian neuronal growth cone revealed using new methods. *Proc Japan Acad Ser B*. 2019;95:358–77.
- Nozumi M, Togano T, Takahashi-Niki K, Lu J, Honda A, Taoka M, Shinkawa T, Koga H, Takeuchi K, Isobe T, Igarashi M. Identification of functional marker proteins in the mammalian growth cone. *Proc Natl Acad Sci U S A*. 2009;106:17211–6.
- Igarashi M. Proteomic identification of the molecular basis of mammalian CNS growth cones. *Neurosci Res*. 2014;88C:1–15.
- Nozumi M, Nakatsu F, Katoh K, Igarashi M. Coordinated movement of vesicles and actin bundles during nerve growth revealed by Superresolution microscopy. *Cell Rep*. 2017;18:2203–16.
- Honda A, Ito Y, Takahashi-Niki K, Matsushita N, Nozumi M, Tabata H, Takeuchi K, Igarashi M. Extracellular signals induce glycoprotein M6a clustering of lipid rafts and associated signaling molecules. *J Neurosci*. 2017;37:4046–64.
- Honda A, Usui H, Sakimura K, Igarashi M. Ruffy3 is an adapter protein for small GTPases that activates a Rac guanine nucleotide exchange factor to control neuronal polarity. *J Biol Chem*. 2017;292:20936–46.
- Tucker RP. The roles of microtubule-associated proteins in brain morphogenesis: a review. *Brain Res Brain Res Rev*. 1990;15:101–20.
- Maccioni RB, Cambiazo V. Role of microtubule-associated proteins in the control of microtubule assembly. *Physiol Rev*. 1995;75:835–64.
- Halpain S, Dehmelt L. The MAP 1 family of microtubule-associated proteins. *Genome Biol*. 2006;7:224.
- Gonzalez-Billault C, Jimenez-Mateos EM, Caceres A, Diaz-Nido J, Wandosell F, Avila J. Microtubule-associated protein 1B function during normal development, regeneration, and pathological conditions in the nervous system. *J Neurobiol*. 2004;58:48–59.
- Riederer BM. Microtubule-associated protein 1B, a growth-associated and phosphorylated scaffold protein. *Brain Res Bull*. 2007;71:541–58.
- Villarreal-Campos D, Gonzalez-Billault C. The MAP 1B case: an old MAP that is new again. *Dev Neurobiol*. 2014;74:953–71.
- Sato-Yoshitake R, Shiomura Y, Miyasaka H, Hirokawa N. Microtubule-associated protein 1B: molecular structure, localization, and phosphorylation-dependent expression in developing neurons. *Neuron*. 1989;3:229–38.
- Black MM, Slaughter T, Fischer I. Microtubule-associated protein 1b (MAP 1b) is concentrated in the distal region of growing axons. *J Neurosci*. 1994;14:857–70.
- Dehmelt L, Halpain S. Actin and microtubules in neurite initiation: are MAPs the missing link? *J Neurobiol*. 2004;58:18–33.
- Jiménez-Mateos EM, Wandosell F, Reiner O, Avila J, González-Billault C. Binding of microtubule-associated protein 1B to LIS1 affects the interaction between dynein and LIS1. *Biochem J*. 2005;389:333–41.
- Tortosa E, Galjart N, Avila J, Sayas CL. MAP 1B regulates microtubule dynamics by sequestering EB1/3 in the cytosol of developing neuronal cells. *EMBO J*. 2013;32:1293–306.
- Fischer I, Romano-Clarke G. Changes in microtubule-associated protein MAP 1B phosphorylation during rat brain development. *J Neurochem*. 1990;55:328–33.
- Nothias F, Fischer I, Murray M, Mirman S, Vincent JD. Expression of a phosphorylated isoform of MAP 1B is maintained in adult central nervous system areas that retain capacity for structural plasticity. *J Comp Neurol*. 1996;368:317–34.
- Humphrey SJ, James DE, Mann M. Protein phosphorylation: a major switch mechanism for metabolic regulation. *Trends Endocrinol Metab*. 2015;26:676–87.
- Kawasaki A, Okada M, Tamada A, Okuda S, Nozumi M, Ito Y, Kobayashi D, Yamasaki T, Yokoyama R, Shibata T, Nishina H, Yoshida Y, Fujii Y, Takeuchi K, Igarashi M. Growth Cone Phosphoproteomics Reveals that GAP-43 Phosphorylated by JNK Is a Marker of Axon Growth and Regeneration. *iScience*. 2018;4:190–203.
- Milosevic A, Zecevic N. Developmental changes in human cerebellum: expression of intracellular calcium receptors, calcium-binding proteins, and phosphorylated and nonphosphorylated neurofilament protein. *J Comp Neurol*. 1998;396:442–60.
- Shin JE, Geisler S, DiAntonio A. Dynamic regulation of SCG10 in regenerating axons after injury. *Exp Neurol*. 2014;252:1–11.
- Eto K, Kawachi T, Osawa M, Tabata H, Nakajima K. Role of dual leucine zipper-bearing kinase (DLK/MUK/ZPK) in axonal growth. *Neurosci Res*. 2010;66:37–45.
- Yamasaki T, Kawasaki H, Arakawa S, Shimizu K, Shimizu S, Reiner O, Okano H, Nishina S, Azuma N, Penninger JM, Katada T, Nishina H. Stress-activated protein kinase MKK7 regulates axon elongation in the developing cerebral cortex. *J Neurosci*. 2011;31:16872–83.
- Feltrin D, Fusco L, Witte H, Moretti F, Martin K, Letzelter M, Fluri E, Scheiffele P, Pertz O. Growth cone MKK7 mRNA targeting regulates MAP 1b-dependent microtubule bundling to control neurite elongation. *PLoS Biol*. 2012;10:e1001439.
- Ulloa L, Avila J, Díaz-Nido J. Heterogeneity in the phosphorylation of microtubule-associated protein MAP 1B during rat brain development. *J Neurochem*. 1993;61:961–72.
- Ulloa L, Díez-Guerra FJ, Avila J, Díaz-Nido J. Localization of differentially phosphorylated isoforms of microtubule-associated protein 1B in cultured rat hippocampal neurons. *Neuroscience*. 1994;61:211–23.
- Shea TB, Majocha RE, Marotta CA, Nixon RA. Soluble, phosphorylated forms of the high molecular weight neurofilament protein in perikarya of cultured neuronal cells. *Neurosci Lett*. 1988;92:291–7.
- Johnstone M, Goold RG, Bei D, Fischer I, Gordon-Weeks PR. Localisation of microtubule-associated protein 1B phosphorylation sites recognised by monoclonal antibody SMI-31. *J Neurochem*. 1997;69:1417–24.
- Del Río JA, González-Billault C, Ureña JM, Jiménez EM, Barallobre MJ, Pascual M, Pujadas L, Simó S, La Torre A, Wandosell F, Avila J, Soriano E. MAP 1B is required for Netrin 1 signaling in neuronal migration and axonal guidance. *Curr Biol*. 2004;14:840–50.
- Goold RG, Owen R, Gordon-Weeks PR. Glycogen synthase kinase 3 β phosphorylation of microtubule-associated protein 1B regulates the stability of microtubules in growth cones. *J Cell Sci*. 1999;112:3373–84.
- Leibinger M, Andreadaki A, Golla R, Levin E, Hilla AM, Diekmann H, Fischer D. Boosting CNS axon regeneration by harnessing antagonistic effects of GSK3 activity. *Proc Natl Acad Sci U S A*. 2017;114:E5454–63.
- Doron-Mandel E, Fainzilber M, Terenzio M. Growth control mechanisms in neuronal regeneration. *FEBS Lett*. 2015;589:1669–77.
- Oyamatsu H, Koga D, Igarashi M, Shibata M, Ushiki T. Morphological assessment of early axonal regeneration in end-to-side nerve coaptation models. *J Plast Surg Hand Surg*. 2012;46:299–307.
- Ma D, Connors T, Nothias F, Fischer I. Regulation of the expression and phosphorylation of microtubule-associated protein 1B during regeneration of adult dorsal root ganglion neurons. *Neuroscience*. 2000;99:157–70.
- Soares S, Barnat M, Salim C, von Boxberg Y, Ravaille-Veron M, Nothias F. Extensive structural remodeling of the injured spinal cord revealed by phosphorylated MAP 1B in sprouting axons and degenerating neurons. *Eur J Neurosci*. 2007;26:1446–61.
- Shah SH, Goldberg JL. The role of axon transport in Neuroprotection and regeneration. *Dev Neurobiol*. 2018;78:998–1010.
- Mori N, Morii H. SCG10-related neuronal growth-associated proteins in neural development, plasticity, degeneration, and aging. *J Neurosci Res*. 2002;70:264–73.
- Chauvin S, Sobel A. Neuronal stathmins: a family of phosphoproteins cooperating for neuronal development, plasticity and regeneration. *Prog Neurobiol*. 2015;126:1–18.
- Riederer BM, Pellier V, Antonsson B, Di Paolo G, Stimpson SA, Lütjens R, Catsicas S, Grenningloh G. Regulation of microtubule dynamics by the neuronal growth-associated protein SCG10. *Proc Natl Acad Sci U S A*. 1997;94:741–5.
- Lütjens R, Igarashi M, Pellier V, Blasey H, Di Paolo G, Ruchti E, Pfulg C, Staple JK, Catsicas S, Grenningloh G. Localization and targeting of SCG10 to the trans-Golgi apparatus and growth cone vesicles. *Eur J Neurosci*. 2000;12:2224–34.
- Togano T, Kurachi M, Watanabe M, Grenningloh G, Igarashi M. Role of Ser50 phosphorylation in SCG10 regulation of microtubule depolymerization. *J Neurosci Res*. 2005;80:475–80.
- Tararuk T, Ostman N, Li W, Björklom B, Padzik A, Zdrojewska J, Hongisto V, Herdegen T, Konopka W, Courtney MJ, Coffey ET. JNK1 phosphorylation of SCG10 determines microtubule dynamics and axodendritic length. *J Cell Biol*. 2006;173:265–77.
- Morii H, Shiraishi-Yamaguchi Y, Mori N. SCG10, a microtubule destabilizing factor, stimulates the neurite outgrowth by modulating microtubule

- dynamics in rat hippocampal primary cultured neurons. *J Neurobiol.* 2006; 66:1101–14.
46. Xu H, Dhanasekaran DN, Lee CM, Reddy EP. Regulation of neurite outgrowth by interactions between the scaffolding protein, JNK-associated leucine zipper protein, and neuronal growth-associated protein superior cervical ganglia clone 10. *J Biol Chem.* 2010;285:3548–53.
 47. Biswas S, Kalil K. The microtubule-associated protein tau mediates the Organization of Microtubules and Their Dynamic Exploration of actin-rich Lamellipodia and Filopodia of cortical growth cones. *J Neurosci.* 2018;38: 291–307.
 48. Igarashi M, Nozumi M, Wu LG, Cella Zancchi F, Katona I, Barna L, Xu P, Zhang M, Xue F, Boyden E new observations in neuroscience using superresolution microscopy. *J Neurosci.* 2018;38:9459–67.
 49. Igarashi M, Okuda S. Evolutionary analysis of proline-directed phosphorylation sites in the mammalian growth cone identified using phosphoproteomics. *Mol Brain.* 2019;12:53.
 50. Tan CSH. Databases and computational tools for evolutionary analysis of protein phosphorylation. *Methods Mol Biol.* 1636;2017:475–84.
 51. Tögel M, Wiche G, Propst F. Novel features of the light chain of microtubule-associated protein MAP 1B: microtubule stabilization, self interaction, actin filament binding, and regulation by the heavy chain. *J Cell Biol.* 1998;143:695–707.
 52. Kiss A, Fischer I, Kleele T, Misgeld T, Propst F. Neuronal growth cone size-dependent and -independent parameters of microtubule polymerization. *Front Cell Neurosci.* 2018;12:195.
 53. Jaskolski F, Mülle C, Manzoni OJ. An automated method to quantify and visualize colocalized fluorescent signals. *J Neurosci Methods.* 2005;146:42–9.
 54. Shelanski ML, Gaskin F, Cantor CR. Microtubule assembly in the absence of added nucleotides. *Proc Natl Acad Sci U S A.* 1973;70:765–8.
 55. Savastano LE, Laurito SR, Fitt MR, Rasmussen JA, Gonzalez-Polo V, Patterson SI. Sciatic nerve injury: a simple and subtle model for investigating many aspects of nervous damage and recovery. *J Neurosci Methods.* 2014;227: 166–80.

Publisher's Note

Springer Nature remains neutral with regard to jurisdictional claims in published maps and institutional affiliations.

Ready to submit your research? Choose BMC and benefit from:

- fast, convenient online submission
- thorough peer review by experienced researchers in your field
- rapid publication on acceptance
- support for research data, including large and complex data types
- gold Open Access which fosters wider collaboration and increased citations
- maximum visibility for your research: over 100M website views per year

At BMC, research is always in progress.

Learn more biomedcentral.com/submissions

